NATIONAL ADVISORY COMMITTEE
FOR AERONAUTICS

JUL 31 1947

TECHNICAL NOTE

No. 1382

DISTRIBUTION OF WAVE DRAG AND LIFT IN THE VICINITY

OF WING TIPS AT SUPERSONIC SPEEDS

By John C. Evvard

Flight Propulsion Research Laboratory
Cleveland, Ohio

NACA

Washington
July 1947

NATIONAL ADVISORY COMMITTEE FOR AERONAUTICS

TECHNICAL NOTE No. 1382

DISTRIBUTION OF WAVE DRAG AND LIFT IN THE VICINITY

OF WING TIPS AT SUPERSONIC SPEEDS

By John C. Evvard

SUMMARY

The point-source-distribution method of calculating the
aerodynamic coefficients of thin wings at supersonic speeds was
extended to include the effect of the region between the wing
boundary and the foremost Mach wave from the wing leading edge.
The effect of this region on the surface velocity potential has
been determined by an equivalent function, which is evaluated
over a portion of the wing surface. In this manner, the effect
of angles of attack and yaw as well as the asymmetry of top and
bottom wing surfaces may be calculated. As examples of the method,
the pressure distribution on a thin plate wing of rectangular plan
form as well as the lift and the drag coefficients as a function
of Mach number, angle of attack, and aspect ratio are calculated.
The equations for the surface velocity potential of several other
plan forms are also included.

INTRODUCTION

The theoretical and experimental investigations of aircraft
performance at supersonic speeds have been greatly stimulated by
modern developments in high-speed flight. The theoretical aero-
dynamic performance of thin wings nevertheless has not been com-
pletely solved, even through the approximations of the linearized
Prandtl-Glauert equation.

Puckett (reference 1), by means of a point source distribu-
tion, has formulated a method to derive the pressure distribution,
the wave lift, and the wave drag for thin wings at angle of
attack, provided that the leading edge or the wing tip, as the
case may be, is swept ahead of the Mach line. The method gener-
ally fails when the sweepback is greater than the Mach line
because the flow over one surface of the wing can influence the
flow on the other surface.

Jones (reference 2) has been able to calculate the pressure
distributions on a series of supersonic wings by means of line
sources. The results are the same as would be obtained by
Puckett's theory, however, and the method is subject to the same
limitations.

After transforming the Prandtl-Glauert equation to curvi-
linear coordinates, Stewart (reference 3) picked the special
solutions corresponding to conical flows. In this manner, the
Prandtl-Glauert equation was reduced to the two-dimensional
Laplace equation that permits the use of conformal mapping. As
a special case, Stewart obtained the lift distribution on a thin
delta wing at small angles of attack. Brown (reference 4) has
independently solved the same problem by use of a doublet line
source distribution on the wing surface.

The present paper extends the point-source-distribution
method (applied by Puckett to the wing surface) to include the
effect of the region between the wing boundary and the foremost
Mach wave from the leading edge. By use of a source distribution
external to the wing, the interaction of the two wing surfaces
may be isolated. In this manner the pressure distribution in the
vicinity of the wing tip, as well as the effect of profile shape,
angles of attack and yaw, and aspect ratio, may be calculated for
a series of finite wings. This work was performed during February
1947 at the NACA Cleveland laboratory.

ANALYSIS OF METHOD

Thin wings will be so used in the analysis that the perturba-
tion velocity components may be assumed to be small compared to
the free-stream velocity. The linearized partial differential
equation for the velocity potential of a compressible fluid may
then be applied. The problem is to find a perturbation velocity
potential that will: (a) satisfy the linearized partial differ-
ential equation of the flow, (b) vanish in the region ahead of
the foremost Mach wave, (c) give streamlines that are tangent to
the airfoil surfaces, and (d) take into account the interaction
between the top and bottom wing surfaces as represented by the
perturbed field between the wing boundary and the foremost Mach
wave.

The Prandtl-Glauert linearized equation for the velocity potential of a nonviscous irrotational compressible fluid may be written as

$$(1 - M^2) \frac{\partial^2 \varphi}{\partial x^2} + \frac{\partial^2 \varphi}{\partial y^2} + \frac{\partial^2 \varphi}{\partial z^2} = 0 \qquad (1)$$

where

M   free-stream Mach number (undisturbed flow parallel to x-axis)

φ perturbation velocity potential

x or ξ
y or η Cartesian coordinates
z or ζ

For convenience the symbols are defined in appendix A. A basic solution for the potential of a unit point source disturbance at (ξ, η, ζ) is

$$\varphi = \frac{-1}{\sqrt{(x - \xi)^2 - \beta^2 (y - \eta)^2 - \beta^2 (z - \zeta)^2}} \qquad (2)$$

where

$$\beta = \sqrt{M^2 - 1}$$

More general solutions may be obtained by integration to give

$$\varphi = -\int\int\int \frac{q' d\xi \, d\eta d\zeta}{\sqrt{(x - \xi)^2 - \beta^2 (y - \eta)^2 - \beta^2 (z - \zeta)^2}} \qquad (3)$$

where q' is the source strength per unit volume. For the thin wing, the sources and the wing may lie in the x, y plane and thus $q' d\zeta$ may be replaced by q, the source strength per unit area. Equation (3) then becomes

$$\varphi = - \iint \frac{q\,d\xi\,d\eta}{\sqrt{(x - \xi)^2 - \beta^2 (y - \eta)^2 - \beta^2 z^2}} \qquad (4)$$

Puckett (reference 1) has shown that the boundary conditions for thin wings may be satisfied as $z \to 0$ by setting $q = w/\pi$, where w is the perturbation velocity component normal to the x, y plane. The quantity w is proportional to the local slope (the angle subtended by the wing surface from the x, y plane in $\eta = $ constant planes) of the wing in the free-stream direction at the point (ξ, η). If λ represents this slope,

$$q = \frac{w}{\pi} = \frac{\lambda U}{\pi} \qquad (5)$$

where U is the free-stream velocity. Equation (4) then becomes

$$\varphi = - \frac{U}{\pi} \iint \frac{\lambda\,d\xi\,d\eta}{\sqrt{(x - \xi)^2 - \beta^2 (y - \eta)^2}} \qquad (6)$$

The form and the derivation of equation (6) indicates that alteration of the local slope λ_1 at point (ξ_1, η_1) will not change the perturbation velocity component w at some other point (ξ, η). The velocity potential at any point (x, y) on the surface of the wing may then be calculated by integrating equation (6) over the region in the x, y plane bounded by the forward Mach cones. (See, for example, fig. 1(b).) Puckett restricted his integration to the wing surface, where λ is assumed known. The solutions obtained in this manner are valid if the wing is swept less than the Mach angle or if the top and bottom surfaces of the wing for any sweepback angle are symmetrical about the x, y plane.

If a proper distribution of source strength $\lambda U/\pi$ is chosen for the regions between the foremost Mach wave and the leading edge, equation (6) will give the velocity potential at any point $(x, y, 0)$ regardless of sweepback angle and asymmetry of top and bottom wing surfaces.

The strength of the source distribution between the Mach cone and the leading edge (or wing tip) must correspond to the

local perturbation velocity component w of the region. This velocity is in turn influenced by the slope of both the top and the bottom surfaces of the wing.

A thin impermeable diaphragm is assumed to coincide with a stream sheet in the x, y plane between the wing surface and the foremost Mach wave. The presence of the diaphragm will not alter the flow over the wing surface. The diaphragm may then be regarded as an extension of the wing to eliminate the external field between the wing boundary and the foremost Mach wave.

Because the diaphragm coincides with a stream sheet, it may sustain no pressure difference at any point between its top and bottom surfaces. Furthermore, there can be no discontinuity in the velocity components across the diaphragm. This situation requires that the surface velocity potential at any point on the top and bottom surfaces of the diaphragm are equal. Inasmuch as the extended wing allows no interaction between its two surfaces, the velocity potential at any point (x, y) may be calculated from either the top or the bottom surface of the original wing and diaphragm.

The local slopes of the wing on its top and bottom surfaces at the point (ξ, η) may be represented by σ_T and σ_B, and λ may represent the corresponding slope on the top surface of the diaphragm. (For convenience, the sign of σ is oppositely defined on the two surfaces. For example, σ_T and σ_B are both positive on a wedge profile at an angle of attack of 0.) The areas of the wing and the diaphragm surfaces included in the forward Mach cone from a point on either the wing or the diaphragm are represented as S_w and S_D, respectively. Number subscripts 1, 2, · · · represent sections of each of these areas. Then by equation (6), the velocity potential at (x_D, y_D) (fig. 1(a)) is

$$\varphi_{D,T} = - \frac{U}{\pi} \iint_{S_W} \frac{\sigma_T d\xi \, d\eta}{\sqrt{(x_D - \xi)^2 - \beta^2 (y_D - \eta)^2}} - \frac{U}{\pi} \iint_{S_D} \frac{\lambda(\xi, \eta) \, d\xi \, d\eta}{\sqrt{(x_D - \xi)^2 - \beta^2 (y_D - \eta)^2}}$$

$$= \varphi_{D,B} = - \frac{U}{\pi} \iint_{S_W} \frac{\sigma_B d\xi \, d\eta}{\sqrt{(x_D - \xi)^2 - \beta^2 (y_D - \eta)^2}} - \frac{U}{\pi} \iint_{S_D} \frac{-\lambda(\xi, \eta) \, d\xi \, d\eta}{\sqrt{(x_D - \xi)^2 - \beta^2 (y_D - \eta)^2}}$$

where $\varphi_{D,T}$ and $\varphi_{D,B}$ are the potentials on the diaphragm calculated from the top and the bottom surfaces of the wing and the diaphragm, respectively. Or

$$\iint_{S_D} \frac{\lambda(\xi, \eta) \, d\xi \, d\eta}{\sqrt{(x_D - \xi)^2 - \beta^2 (y_D - \eta)^2}} = \iint_{S_W} \frac{(\sigma_B - \sigma_T) \, d\xi \, d\eta}{2\sqrt{(x_D - \xi)^2 - \beta^2 (y_D - \eta)^2}} \tag{7}$$

This integral equation defines the function λ. The velocity potential at any point (x, y) on the top surface of the wing is given from equation (6) as

$$\varphi_T = - \frac{U}{\pi} \iint_{S_W} \frac{\sigma_T d\xi \, d\eta}{\sqrt{(x - \xi)^2 - \beta^2 (y - \eta)^2}} - \frac{U}{\pi} \iint_{S_D} \frac{\lambda(\xi, \eta) \, d\xi \, d\eta}{\sqrt{(x - \xi)^2 - \beta^2 (y - \eta)^2}} \tag{8}$$

Similarly, the potential on the bottom surface is

$$\varphi_B = - \frac{U}{\pi} \iint_{S_W} \frac{\sigma_B d\xi \, d\eta}{\sqrt{(x - \xi)^2 - \beta^2 (y - \eta)^2}} + \frac{U}{\pi} \iint_{S_D} \frac{\lambda(\xi, \eta) \, d\xi \, d\eta}{\sqrt{(x - \xi)^2 - \beta^2 (y - \eta)^2}} \tag{8a}$$

where the integration is made over the region in the x, y plane bounded by the forward Mach cone from the point (x, y) over all wing and diaphragm surfaces.

In special cases, the potential φ of equation (8) may be obtained without explicitly solving for λ. This simplification is most easily accomplished in an oblique u, v coordinate system the axes of which lie parallel to the Mach waves. In this system, for example, the value of the coordinate u is the distance from the v-axis to the point measured parallel to the u-axis. The transformation equations are

$$u = \frac{M}{2\beta} (\xi - \beta\eta) \qquad\qquad v = \frac{M}{2\beta} (\xi + \beta\eta)$$

$$\xi = \frac{\beta}{M} (v + u) \qquad\qquad \eta = \frac{1}{M} (v - u) \qquad\qquad (9)$$

Inasmuch as the elemental area in the u, v coordinate system is $\frac{2\beta}{M^2} \, du \, dv$, equation (7) may be written either as

$$\frac{2\beta}{M^2} \iint_{S_D} \frac{\lambda(u, v) \, du \, dv}{\sqrt{\left[x_D - \frac{\beta}{M}(v + u)\right]^2 - \beta^2 \left[y_D - \frac{1}{M}(v - u)\right]^2}} = \frac{2\beta}{M^2} \iint_{S_W} \frac{(\sigma_B - \sigma_T) \, du \, dv}{2\sqrt{\left[x_D - \frac{\beta}{M}(v + u)\right]^2 - \beta^2 \left[y_D - \frac{1}{M}(v - u)\right]^2}}$$

$$(7a)$$

or as

$$\frac{1}{M} \iint_{S_D} \frac{\lambda(u, v) \, du \, dv}{\sqrt{(u_D - u)(v_D - v)}} = \frac{1}{M} \iint_{S_W} \frac{(\sigma_B - \sigma_T) \, du \, dv}{2\sqrt{(u_D - u)(v_D - v)}} \tag{7b}$$

where u_D and v_D represent the coordinates of the point (x_D, y_D) in the u, v system.

The regions of integration and the coordinate systems of equation (7) are sketched for a wing plan view in figure 1(a). The zero of the coordinate system is placed at the point of tangency of the foremost Mach wave and the leading edge. The wing area S_w is bounded by the two curves (or two branches of the same curve) $v = v_1(u)$ and $v = v_2(u)$ and the line $u = u_D = \frac{M}{2\beta}(x_D - \beta y_D)$. Application of equation 7(b) to this case yields

$$\int_0^{u_D} \frac{du}{\sqrt{(u_D - u)}} \int_{v_2(u)}^{v_D} \frac{\lambda(u, v) \, dv}{\sqrt{(v_D - v)}} = \int_0^{u_D} \frac{du}{\sqrt{(u_D - u)}} \int_{v_1(u)}^{v_2(u)} \frac{(\sigma_B - \sigma_T)}{2} \frac{dv}{\sqrt{(v_D - v)}} \tag{10}$$

Inasmuch as the limits of integration of the $\dfrac{du}{\sqrt{(u_D - u)}}$ integrals are the same for all values of u_D and owing to the nature of the functions, the two integrations with respect to v may be equated along lines of constant v_D that extend across the wing and the diaphragm.

$$\int_{v_2(u)}^{v_D} \frac{\lambda(u, v) \, dv}{\sqrt{(v_D - v)}} = \int_{v_1(u)}^{v_2(u)} \frac{(\sigma_B - \sigma_T)}{2} \frac{dv}{\sqrt{(v_D - v)}} \tag{11}$$

The contribution to the velocity potential on the top surface of the wing attributed to the diaphragm (fig. 1(b)) is given by equations (8) and (9) as

$$\varphi_{T,D} = - \frac{U}{M\pi} \int_0^{u'} \frac{du}{\sqrt{(u_W - u)}} \int_{v_2(u)}^{v_W} \frac{\lambda(u, v) \, dv}{\sqrt{(v_W - v)}} \tag{12}$$

where u_W and v_W are the coordinates of point (x, y) on the wing and the limit u' is obtained by solving the equation

$$v_W = v_2 (u')$$

The integration limits with respect to v and the integrand of equation (12) are the same as the left side of equation (11), except that v_W replaces v_D; but the value of v_D along the $v = \text{constant}$ line passing through the point (u_W, v_W) is v_W. The second member of equation (11) may therefore be substituted into equation (12) to give

$$\varphi_{T,D} = - \frac{U}{M\pi} \int_0^{u'} \frac{du}{\sqrt{(u_W - u)}} \int_{v_1(u)}^{v_2(u)} \frac{(\sigma_B - \sigma_T)}{2} \frac{dv}{\sqrt{(v_W - v)}}$$

$$= - \frac{U}{\pi} \iint_{S_{W,2}} \frac{(\sigma_B - \sigma_T) \, d\xi \, d\eta}{2\sqrt{(x - \xi)^2 - \beta^2(y - \eta)^2}} \tag{13}$$

The contribution of the diaphragm to the potential on the wing surface may thus be replaced by an equivalent integration over a portion of the wing surface. The potential on the wing surface is then

$$\varphi_T = \varphi_{T,D} + \varphi_{T,W} = -\frac{U}{\pi}\iint_{S_{W,2}} \frac{(\sigma_B - \sigma_T)\,d\xi\,d\eta}{2\sqrt{(x-\xi)^2 - \beta^2(y-\eta)^2}}$$

$$-\frac{U}{\pi}\iint_{S_{W,2}} \frac{\sigma_T\,d\xi\,d\eta}{\sqrt{(x-\xi)^2 - \beta^2(y-\eta)^2}}$$

$$-\frac{U}{\pi}\iint_{S_{W,1}} \frac{\sigma_T\,d\xi\,d\eta}{\sqrt{(x-\xi)^2 - \beta^2(y-\eta)^2}}$$

$$= -\frac{U}{\pi}\iint_{S_{W,1}} \frac{\sigma_T\,d\xi\,d\eta}{\sqrt{(x-\xi)^2 - \beta^2(y-\eta)^2}}$$

$$-\frac{U}{\pi}\iint_{S_{W,2}} \frac{(\sigma_B + \sigma_T)\,d\xi\,d\eta}{2\sqrt{(x-\xi)^2 - \beta^2(y-\eta)^2}} \tag{14}$$

or

$$\varphi_T = -\frac{2\beta U}{\pi M^2}\iint_{S_{W,1}} \frac{\sigma_T\,du\,dv}{\sqrt{\left[x - \frac{\beta}{M}(v+u)\right]^2 - \beta^2\left[y - \frac{1}{M}(v-u)\right]^2}}$$

$$-\frac{2\beta U}{\pi M^2}\iint_{S_{W,2}} \frac{(\sigma_B + \sigma_T)\,du\,dv}{2\sqrt{\left[x - \frac{\beta}{M}(v+u)\right]^2 - \beta^2\left[y - \frac{1}{M}(v-u)\right]^2}} \tag{14a}$$

The derivation of equation (13) includes the assumptions of the linearized theory and the assumption that the leading edge is not blunt (corresponding to the use of a thin diaphragm). Aside from these restrictions, the equation includes the effect of asymmetry between the top and the bottom wing surfaces. It may therefore be applied to determine wave lift, drag, and pressure distribution in

the vicinity of wing tips of fairly general chordwise slope dis-
tributions. Because the only restriction on the functions $v_1 (u)$
and $v_2 (u)$ was that S_D be influenced only by the wing sec-
tion S_W, the aerodynamic properties of fairly general plan forms
may be evaluated. (In cases of so-called subsonic trailing edges,
the solution for the velocity potential that is obtained vio-
lates the Kutta-Joukowski condition in the vicinity of the trail-
ing edge. The solutions may not correspond to actual flows under
these conditions.) The effect of yawing the wing may also be
determined simply by simultaneously adjusting the functions $v_1 (u)$,
$v_2 (u)$, σ_B, and σ_T by an amount corresponding to the angle of
yaw. The effectiveness of wing tips and hence the effect of aspect
ratio may likewise be determined.

EXAMPLES OF METHOD

Thin flat plate wing with rectangular plan form and no sweep
back. - For the flat plate wing (fig. 2), $\sigma_B = -\sigma_T =$ angle of
attack α and equation (14) becomes

$$\varphi_T = \frac{U\alpha}{\pi} \iint_{S_{W,1}} \frac{d\xi\, d\eta}{\sqrt{(x - \xi)^2 - \beta^2 (y - \eta)^2}} \tag{15}$$

Thus, the external field S_D cancels the effect of the region $S_{W,2}$
as far as the potential at point (x, y) is concerned.

The pressure coefficient C_p in the region of the wing tip
may be computed from the equation

$$C_p = -\frac{2}{U} \frac{\partial \varphi}{\partial x} \tag{16}$$

The value of C_p' obtained from equations (15) and (16) is derived
in appendix B for the top surface of the wing to give

$$C_{p,T} = -\frac{\alpha}{\beta} + \frac{2\alpha}{\pi\beta} \sin^{-1}\left(\frac{2\beta y}{x} + 1\right) \tag{17}$$

(Equation (17) is equation (B1) in appendix B.) The coordinate y is, of course, negative. The pressure is therefore constant along radial lines from the origin, has the free-stream value along the tip, and has the Ackeret value (reference 5) along the Mach line lying on the wing from the tip and leading edge intersection. If the influence of the external field S_D has been neglected, the pressure coefficient would be one-half the Ackeret value along the wing tip instead of the correct value of 0. The result presented in equation (17) was first derived by Busemann (reference 6) and has been cited in reference 7.

The pressures on the top and bottom surfaces of the region influenced by the wing tip are integrated in appendix B to give the lift and drag coefficients. The lift and drag coefficients are one-half the values obtained by the Ackeret theory (reference 5). The wave lift and drag coefficients for the whole wing are given in terms of the aspect ratio A (if $A \geq \frac{2}{\beta}$) as

$$\left.\begin{array}{l} C_L = \dfrac{4\alpha}{\beta}\left(1 - \dfrac{1}{2\beta A}\right) \\[3mm] C_D = \dfrac{4\alpha^2}{\beta}\left(1 - \dfrac{1}{2\beta A}\right) \end{array}\right\} \tag{18}$$

which is derived as equation (B4) in appendix B. This effect of aspect ratio on the thin flat plate wing has been previously reported in reference 8.

Discontinuously swept wing of small finite thickness except on edges. - The leading edge may lie on lines $v = -k_1 u$, and $v = k_2 u$, where k_1 and k_2 are positive constants. (See fig. 3.) For this case, equation (14a) becomes

$$\varphi_T = -\frac{2U\beta}{\pi M^2}\int_0^{\frac{M}{2\beta k_2}(x+\beta y)} du \int_{-k_1 u}^{k_2 u} \frac{(\sigma_B + \sigma_T)\,dv}{2\sqrt{\left[x - \frac{\beta}{M}(v+u)\right]^2 - \beta^2\left[y - \frac{1}{M}(v-u)\right]^2}}$$

$$-\frac{2U\beta}{\pi M^2}\int_{\frac{M}{2\beta k_2}(x+\beta y)}^{\frac{M}{2\beta}(x-\beta y)} du \int_{-k_1 u}^{\frac{M}{2\beta}(x+\beta y)} \frac{\sigma_T\,dv}{\sqrt{\left[x - \frac{\beta}{M}(v+u)\right]^2 - \beta^2\left[y - \frac{1}{M}(v-u)\right]^2}}$$

$$\tag{19}$$

Similarly, the potential on the bottom of the wing is

$$\varphi_B = - \frac{2U\beta}{\pi M^2} \int_C^{\frac{M}{2\beta k_2}(x+\beta y)} du \int_{-k_1 u}^{k_2 u} \frac{(\sigma_B + \sigma_T)\ dv}{2\sqrt{\left[x - \frac{\beta}{M}(v+u)\right]^2 - \beta^2\left[y - \frac{1}{M}(v-u)\right]^2}}$$

$$- \frac{2U\beta}{\pi M^2} \int_{\frac{M}{2\beta k_2}(x+\beta y)}^{\frac{M}{2\beta}(x-\beta y)} du \int_{-k_1 u}^{\frac{M}{2\beta}(x+\beta y)} \frac{\sigma_B\ dv}{\sqrt{\left[x - \frac{\beta}{M}(v+u)\right]^2 - \beta^2\left[y - \frac{1}{M}(v-u)\right]^2}}$$

(19a)

Equations (19) and (19a) apply for wings at angles of attack even though the top and bottom surfaces are asymmetrical. For symmetrical profiles at an angle of attack of 0, they reduce to the expressions obtained by Puckett's theory.

An interesting observation is that only the second of the two integrals in equations (19) and (19a) includes the effect of angle of attack; at an angle of attack α, $\sigma_B = \sigma_B' + \alpha$, $\sigma_T = \sigma_T' - \alpha$, and $\sigma_B + \sigma_T = \sigma_B' + \sigma_T'$, where σ_B' and σ_T' are the local wing slopes on the bottom and top surfaces at an angle of attack of 0. The first integrals of equations (19) and (19a) are identical. Therefore, only the second integral contributes to $\frac{\partial C_L}{\partial \alpha}$. Both integrals must be considered when pressure distribution or drag coefficients are desired.

As an example of the use of equation (19), the velocity potential for a wedge wing (fig. 4) of constant wedge angle 2σ parallel to the free-stream direction has been calculated in appendix C as equation (C2). This potential for the top surface of the wing is

$$\varphi_T = \frac{U\sigma}{\pi\beta}\left\{ - \frac{\left[(1 + k_1)\, x + (1 - k_1)\right]\beta y}{\sqrt{k_1}}\, \tan^{-1}\sqrt{\frac{k_1\,(x - \beta y)}{(x + \beta y)}}\right.$$

$$\left. + \frac{\left[(k_2 - 1)\, x - (k_2 + 1)\,\beta y\right]}{\sqrt{k_2}}\, \log\, \frac{\sqrt{(k_2 - 1)\, x - (k_2 + 1)\,\beta y}}{\sqrt{k_2\,(x - \beta y)} + \sqrt{x + \beta y}}\right\}$$

$$+ \frac{U\alpha}{\pi\beta}\left\{\sqrt{\frac{(k_1 + k_2)\,(x + \beta y)\left[(k_2 - 1)\, x - (k_2 + 1)\,\beta y\right]}{k_2{}^2}}\right.$$

$$\left. + \frac{(1 + k_1)\, x + (1 - k_1)\,\beta y}{\sqrt{k_1}}\, \tan^{-1}\sqrt{\frac{k_1\left[(k_2 - 1)\, x - (k_2 + 1)\,\beta y\right]}{(k_1 + k_2)\,(x + \beta y)}}\right\} \tag{20}$$

The velocity potential for the bottom surface may be obtained by replacing α by $-\alpha$. Only the second brace of equation (20) influences the lift of the wing. Pressure coefficients may be obtained by substituting equation (20) into equation (16).

Wing influenced by two independent perturbed flow fields external to wing surface. - An external flow field is considered to be independent if it does not include an external flow field of unknown strength in its forward Mach cone. (See fig. 5.) If

$$K\,(x,\ y,\ \xi,\ \eta) \equiv \frac{U}{\pi\sqrt{(x - \xi)^2 - \beta^2\,(y - \eta)^2}}$$

the velocity potential at point $(x,\ y)$ will be

$$\varphi_T = - \iint_{S_W} \sigma_T K\, d\xi\, d\eta - \iint_{S_{D,1}} \lambda_1 K\, d\xi\, d\eta$$

$$- \iint_{S_{D,2}} \lambda_2 K\, d\xi\, d\eta \tag{21}$$

By application of equation (13)

$$\iint_{S_{D,1}} \lambda_1 K d\xi \, d\eta = \iint_{S_{w,1}} \frac{(\sigma_B - \sigma_T) K}{2} \, d\xi \, d\eta$$

$$+ \iint_{S_{w,2}} \frac{(\sigma_B - \sigma_T) K}{2} \, d\xi \, d\eta \qquad (22)$$

and

$$\iint_{S_{D,2}} \lambda_2 K d\xi \, d\eta = \iint_{S_{w,3}} \frac{(\sigma_B - \sigma_T) K}{2} \, d\xi \, d\eta$$

$$+ \iint_{S_{w,2}} \frac{(\sigma_B - \sigma_T) K}{2} \, d\xi \, d\eta \qquad (23)$$

Also

$$\iint_{S_w} \sigma_T K d\xi \, d\eta = \iint_{S_{w,1}} \sigma_T K d\xi \, d\eta + \iint_{S_{w,2}} \sigma_T K d\xi \, d\eta$$

$$+ \iint_{S_{w,3}} \sigma_T K d\xi \, d\eta + \iint_{S_{w,4}} \sigma_T K d\xi \, d\eta \qquad (24)$$

Substitution of equations (22), (23), and (24) into (21) yields

$$\varphi_T = - \iint_{S_{w,1}} \frac{(\sigma_B + \sigma_T) K}{2} d\xi \, d\eta - \iint_{S_{w,2}} \sigma_B K d\xi \, d\eta$$

$$- \iint_{S_{w,3}} \frac{(\sigma_B + \sigma_T) K}{2} d\xi \, d\eta - \iint_{S_{w,4}} \sigma_T K d\xi \, d\eta \quad (21a)$$

Similar extensions may be made for other independently perturbed flow regions in the forward Mach cone. (The boundary of the shaded region in figure 5 gives the limit of validity of equation (21a). The shaded region is influenced by external fields that are no longer independent.)

Because equations (7) and (8) are linear with respect to the local wing slope σ, equations (14), (19), and (21) may be divided into two sets of integrals; the first set will depend on the angle of attack α, but will be independent of the wing slope σ' at an angle of attack of 0; the other set will be independent of angle of attack but will depend on the slope σ'. For symmetrical profiles about the x, y plane (at an angle of attack of 0), the second set consists of the velocity potential for the given plan form at an angle of attack of 0. The first set represents the velocity potential of the thin flat plate wing. For symmetrical profiles at angle of attack, the aerodynamic coefficients for the wing may therefore be obtained by superposing the solution at an angle of attack of 0 (calculated by the methods of Puckett (reference 1) or Jones (reference 2)) and the solution at angle of attack of a thin flat plate wing of the same plan form. From the form of equations (7) and (8), this superposition is apparently general. In this manner, for example, solutions for the symmetrical delta wing and the related airfoils of somewhat arbitrary chordwise thickness distribution may be obtained from the results of Stewart (reference 3) or Brown (reference 4).

DISCUSSION OF METHOD

The general equations (7) and (8) will satisfy the boundary conditions of thin wings at supersonic speeds. The less general solution of equation (13) may be applied to calculate the

contribution to the velocity potential on the wing of a single
perturbed field between the wing boundary and the foremost per-
turbed Mach cone; as illustrated by equation (21a), the method
may be extended to include the effects of a multiplicity of
independently perturbed external flow fields. The basic
equation (8) from which the succeeding equations were derived
includes the effects of asymmetry about the x, y plane between
the top and bottom surfaces, such as would occur at angles of
attack. The method may also be used to calculate the effects
of yawing the wing.

Flight Propulsion Research Laboratory,
        National Advisory Committee for Aeronautics,
                Cleveland, Ohio, May 27, 1947.

APPENDIX A

SYMBOLS

The following symbols are used in this report:

A	aspect ratio
C_D	drag coefficient
C_L	lift coefficient
C_p	pressure coefficient
k_1, k_2	constants greater than zero
M	free-stream Mach number
q	disturbance source strength per unit area
q'	disturbance source strength per unit volume
S	plan form area
U	free-stream velocity

$$\left. \begin{aligned} u &= \frac{M}{2\beta}(\xi - \beta\eta) \\[6pt] v &= \frac{M}{2\beta}(\xi + \beta\eta) \end{aligned} \right\} \quad \text{oblique coordinates whose axes lie parallel to Mach lines}$$

w	z component of perturbation velocity
x, y, z	Cartesian coordinates
x_c	wing chord
α	angle of attack
β	cotangent of free-stream Mach angle, $\sqrt{M^2 - 1}$
ξ, η, ζ	Cartesian coordinates

λ slope of stream sheet near ξ, η plane
                                   measured in η = constant planes

σ slope of the wing surface with respect to the
                                   ξ, η plane measured in η = constant planes

σ' slope of wing surface at zero angle of attack

φ perturbation velocity potential

Subscripts:

B   bottom (wing or diaphragm surface)

T   top (wing or diaphragm surface)

D   diaphragm (with exception of C_D)

w   wing

1, 2, 3   refer either to numbered areas or curves

Examples:

σ_T slope on top wing surface

$\varphi_{T,D}$ potential on top surface of wing due to
                                   diaphragm

$S_{w,3}$ wing area 3

v_1 curve $v = v_1(u)$

λ_1 slope of diaphragm in plan area 1

$C_{p,T}$ pressure coefficient on top surface of wing

APPENDIX B

LIFT DISTRIBUTION NEAR TIP OF THIN WING

OF RECTANGULAR PLAN FORM

The limits of integration of equation (15) are evident from the following sketch.
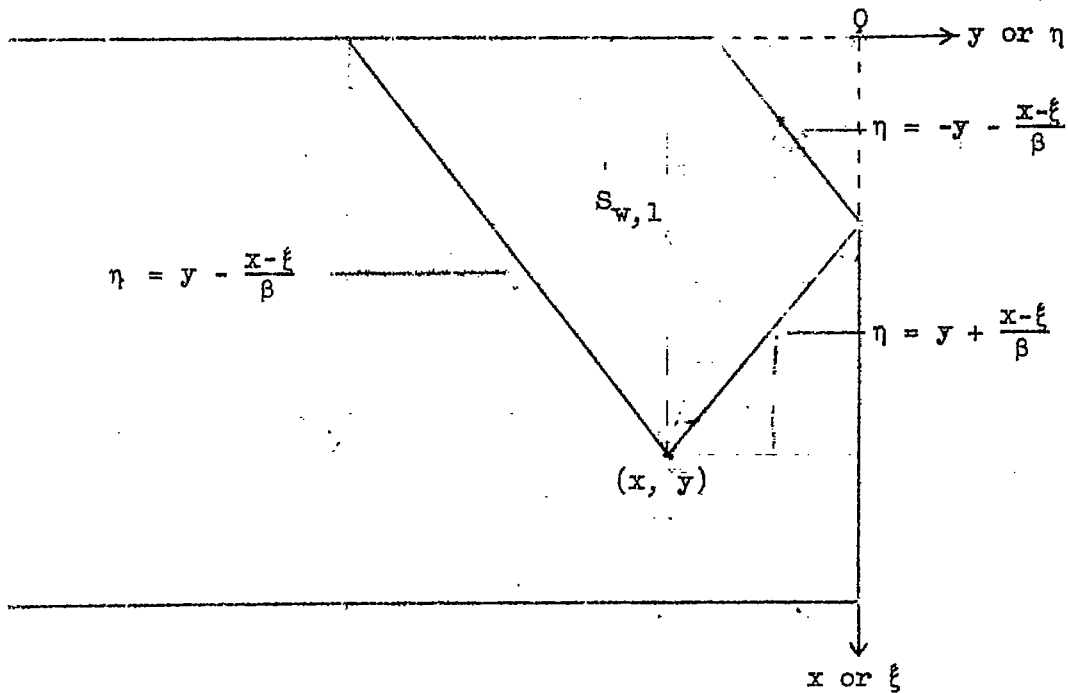
The potential at point (x, y) is then

$$\varphi_T = \frac{U\alpha}{\pi} \int_0^{x+\beta y} d\xi \int_{y-\frac{x-\xi}{\beta}}^{-y-\frac{x-\xi}{\beta}} \frac{d\eta}{\sqrt{(x-\xi)^2 - \beta^2(y-\eta)^2}}$$

$$+ \frac{U\alpha}{\pi} \int_{x+\beta y}^{x} d\xi \int_{y-\frac{x-\xi}{\beta}}^{y+\frac{x-\xi}{\beta}} \frac{d\eta}{\sqrt{(x-\xi)^2 - \beta^2(y-\eta)^2}}$$

$$= -\frac{U\alpha}{\pi\beta} \int_0^{x+\beta y} \left[\sin^{-1}\left(\frac{2\beta y}{x-\xi} + 1\right) - \frac{\pi}{2} \right] d\xi - U\alpha y$$

Partial differentiation with respect to x yields

$$\frac{\partial \varphi_T}{\partial x} = \frac{U\alpha}{2\beta} + \frac{U\alpha}{2\beta} - \frac{U\alpha}{\pi\beta} \int_0^{x+\beta y} \frac{\partial}{\partial x} \sin^{-1}\left(\frac{2\beta y}{x-\xi} + 1\right) d\xi$$

$$= \frac{U\alpha}{2\beta} + \frac{U\alpha}{2\beta} + \frac{U\alpha}{\pi\beta} \int_0^{x+\beta y} \frac{\partial}{\partial \xi} \sin^{-1}\left(\frac{2\beta y}{x-\xi} + 1\right) d\xi$$

$$= \frac{U\alpha}{2\beta} - \frac{U\alpha}{\pi\beta} \sin^{-1}\left(\frac{2\beta y}{x} + 1\right)$$

Therefore from equation (16)

$$C_p = -\frac{2}{U}\frac{\partial \varphi}{\partial x} = -\frac{\alpha}{\beta} + \frac{2\alpha}{\pi\beta} \sin^{-1}\left(\frac{2\beta y}{x} + 1\right) \tag{B1}$$

The average lift coefficient for the wing tip may be computed
for the flat plate wing as

$$C_L = \frac{\int - 2\, C_p\, dS}{\int dS}$$

Because C_p is constant along radial lines from the origin, a
triangular infinitesimal area is convenient. In terms of
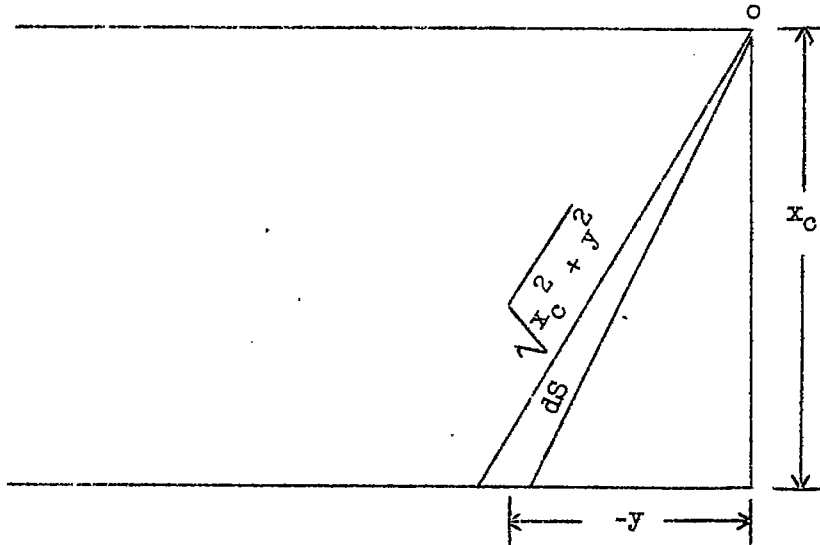
the chord x_c this area is

$$dS = -\frac{x_c\, dy}{2}$$

$$\int - 2\ C_p\ dS = \int_0^{-\frac{x_c}{\beta}} x_c\ C_p\ dy = \int_0^{-\frac{x_c}{\beta}} \left[-\frac{\alpha x_c}{\beta} + \frac{2\alpha x_c}{\pi\beta} \sin^{-1} \left(\frac{2\beta y}{x_c} + 1 \right) \right] dy = \frac{\alpha x_c^2}{\beta^2}$$

Therefore

$$C_L = \frac{2\alpha}{\beta} \tag{B2}$$

and

$$C_D = \frac{2\alpha^2}{\beta} \tag{B3}$$

On the average, the wing tip area is one-half as effective as the rest of the wing, although the lift-drag ratio in the frictionless case is the same. In terms of the aspect ratio A, the wave lift and drag coefficients of the whole wing are

$$C_L = \frac{4\alpha}{\beta} \left(1 - \frac{1}{2\beta A} \right)$$

$$C_D = \frac{4\alpha^2}{\beta} \left(1 - \frac{1}{2\beta A} \right) \tag{B4}$$

APPENDIX C

CALCULATION OF VELOCITY POTENTIAL OF A DISCONTINUOUSLY

SWEPT WEDGE WING

For the wing of wedge angle 2σ shown in figure 4, equation (19) becomes

$$-\frac{\pi M^2 \varphi_T}{2U\beta} = \int_{\frac{M}{2\beta k_2}(x+\beta y)}^{\frac{M}{2\beta}(x-\beta y)} du \int_{-k_1 u}^{\frac{M}{2\beta}(x+\beta y)} \frac{(\sigma - \alpha)\, dv}{\sqrt{\left[x-\frac{\beta}{M}(v+u)\right]^2 - \beta^2\left[y-\frac{1}{M}(v-u)\right]^2}}$$

$$+ \int_{0}^{\frac{M}{2\beta k_2}(x+\beta y)} du \int_{-k_1 u}^{k_2 u} \frac{\sigma\, dv}{\sqrt{\left[x-\frac{\beta}{M}(v+u)\right]^2 - \beta^2\left[y-\frac{1}{M}(v-u)\right]^2}} \quad (C1)$$

$$= -\int_{\frac{M}{2\beta k_2}(x+\beta y)}^{\frac{M}{2\beta}(x-\beta y)} (\sigma-\alpha)\frac{M}{\beta}\left[\sqrt{\frac{x+\beta y - \frac{2\beta v}{M}}{x-\beta y - \frac{2\beta u}{M}}}\right]_{-k_1 u}^{\frac{M}{2\beta}(x+\beta y)} du$$

$$- \int_{0}^{\frac{M}{2\beta k_2}(x+\beta y)} \sigma\frac{M}{\beta}\left[\sqrt{\frac{x+\beta y - \frac{2\beta v}{M}}{x-\beta y - \frac{2\beta u}{M}}}\right]_{-k_1 u}^{k_2 u} du$$

$$= (\sigma-\alpha)\frac{M}{\beta}\int_{\frac{M}{2\beta k_2}(x+\beta y)}^{\frac{M}{2\beta}(x-\beta y)} \sqrt{\frac{x+\beta y + \frac{2\beta k_1 u}{M}}{x-\beta y - \frac{2\beta u}{M}}}\, du$$

$$+ \frac{\sigma M}{\beta} \int_0^{\frac{M}{2\beta k_2}(x+\beta y)} \sqrt{\frac{x+\beta y + \frac{2\beta k_1 u}{M}}{x-\beta y - \frac{2\beta u}{M}}} \; du$$

$$- \frac{\sigma M}{\beta} \int_0^{\frac{M}{2\beta k_2}(x+\beta y)} \sqrt{\frac{x+\beta y - \frac{2\beta k_2 u}{M}}{x-\beta y - \frac{2\beta u}{M}}} \; du$$

$$= \frac{\sigma M}{\beta} \int_0^{\frac{M}{2\beta}(x-\beta y)} \sqrt{\frac{x+\beta y + \frac{2\beta k_1 u}{M}}{x-\beta y - \frac{2\beta u}{M}}} \; du$$

$$- \frac{\sigma M}{\beta} \int_0^{\frac{M}{2\beta k_2}(x+\beta y)} \sqrt{\frac{x+\beta y - \frac{2\beta k_2 u}{M}}{x-\beta y - \frac{2\beta u}{M}}} \; du$$

$$- \alpha \frac{M}{\beta} \int_{\frac{M}{2\beta k_2}(x+\beta y)}^{\frac{M}{2\beta}(x-\beta y)} \sqrt{\frac{x+\beta y + \frac{2\beta k_1 u}{M}}{x-\beta y - \frac{2\beta u}{M}}} \; du$$

Each of these integrals may be integrated (reference 9, integrals 111 and 113), although care should be taken in the choice of signs for the square roots. The following scheme was applied:

$$\sqrt{|b||b'|} = |\sqrt{b\ b'}|$$

$$\sqrt{(-|b|)(-|b'|)} = -|\sqrt{b\ b'}|$$

$$\sqrt{-(-|b|)|b^r|} = +\sqrt{b\ b'}|$$

where b and b' are arbitrary numbers. In other words, when two negative signs are multiplied under the radical, the negative sign is transferred as a factor to the front of the radical. The integrations yield

$$\int_0^{\frac{M}{2\beta}(x-\beta y)} \sqrt{\frac{x+\beta y + \frac{2\beta k_1 u}{M}}{x-\beta y - \frac{2\beta u}{M}}}\ du = \frac{M}{2\beta}\sqrt{x^2-\beta^2 y^2} + \frac{M}{2\beta}\frac{\left[(1+k_1)\ x + (1-k_1)\ \beta y\right]}{\sqrt{k_1}} \tan^{-1}\sqrt{\frac{k_1(x-\beta y)}{(x+\beta y)}}$$

$$\int_0^{\frac{M}{2\beta k_2}(x+\beta y)} \sqrt{\frac{x+\beta y - \frac{2\beta k_2 u}{M}}{x-\beta y - \frac{2\beta u}{M}}}\ du = \frac{-M}{2\beta}\sqrt{x^2-\beta^2 y^2} + \frac{M\left[(k_2-1)x - (k_2+1)\ \beta y\right]}{2\beta\sqrt{k_2}} \log \frac{\sqrt{(k_2-1)x - (k_2+1)\ \beta y}}{\sqrt{k_2(x-\beta y)} + \sqrt{x+\beta y}}$$

$$\int_{\frac{M}{2\beta k_2}(x+\beta y)}^{\frac{M}{2\beta}(x-\beta y)} \sqrt{\frac{x+\beta y + \frac{2\beta k_1 u}{M}}{x-\beta y - \frac{2\beta u}{M}}}\, du = \frac{M}{2\beta}\sqrt{\frac{(k_1+k_2)}{(k_2)^2}(x+\beta y)\left[(k_2-1)\, x - (k_2+1)\, \beta y\right]}$$

$$+ \frac{M}{2\beta}\frac{\left[(1+k_1)x + (1-k_1)\,\beta y\right]}{\sqrt{k_1}}\tan^{-1}\sqrt{\frac{k_1\left[(k_2-1)\, x - (k_2+1)\,\beta y\right]}{(k_1+k_2)\,(x+\beta y)}}$$

Hence

$$\varphi_T = \frac{U\sigma}{\pi\beta}\left\{-\frac{\left[(1+k_1)x + (1-k_1)\beta y\right]}{\sqrt{k_1}}\tan^{-1}\sqrt{\frac{k_1(x-\beta y)}{(x+\beta y)}} + \frac{\left[(k_2-1)x - (k_2+1)\beta y\right]}{\sqrt{k_2}}\log\frac{\sqrt{(k_2-1)x - (k_2+1)\beta y}}{\sqrt{k_2(x-\beta y)} + \sqrt{x+\beta y}}\right\}$$

$$+ \frac{U\alpha}{\pi\beta}\left\{\sqrt{\frac{(k_1+k_2)\,(x+\beta y)\,\left[(k_2-1)x - (k_2+1)\,\beta y\right]}{k_2^{\,2}}}\right.$$

$$\left. + \frac{\left[(1+k_1)x + (1-k_1)\,\beta y\right]}{\sqrt{k_1}}\tan^{-1}\sqrt{\frac{k_1\left[(k_2-1)x - (k_2+1)\,\beta y\right]}{(k_1+k_2)\,(x+\beta y)}}\right\}$$

REFERENCES

1. Puckett, Allen E.: Supersonic Wave Drag of Thin Airfoils.
     Jour. Aero. Sci., vol. 13, no. 9, Sept. 1946, pp. 475-484.

2. Jones, Robert T.: Thin Oblique Airfoils at Supersonic Speed.
     NACA TN No. 1107, 1946.

3. Stewart, H. J.: The Lift of a Delta Wing at Supersonic Speeds.
     Quarterly Appl. Math., vol. IV, no. 3, Oct. 1946, pp. 246-254.

4. Brown, Clinton E.: Theoretical Lift and Drag of Thin Trian-
     gular Wings at Supersonic Speeds. NACA TN No. 1183, 1946.

5. Ackeret, J.: Air Forces on Airfoils Moving Faster than Sound.
     NACA TM No. 317, 1925.

6. Busemann, Adolf: Infinitesimal Conical Supersonic Flow. NACA
     TM No. 1100, 1947.

7. Bonney, E. Arthur: Aerodynamic Characteristics of Rectangular
     Wings at Supersonic Speeds. Jour. Aero. Sci., vol. 14, no. 2,
     Feb. 1947, pp. 110-116.

8. Lighthill, M. J.: The Supersonic Theory of Wings of Finite
     Span. R. & M. No. 2001, British A. R. C., 1944.

9. Peirce, B. O.: A Short Table of Integrals. Ginn and Co.,
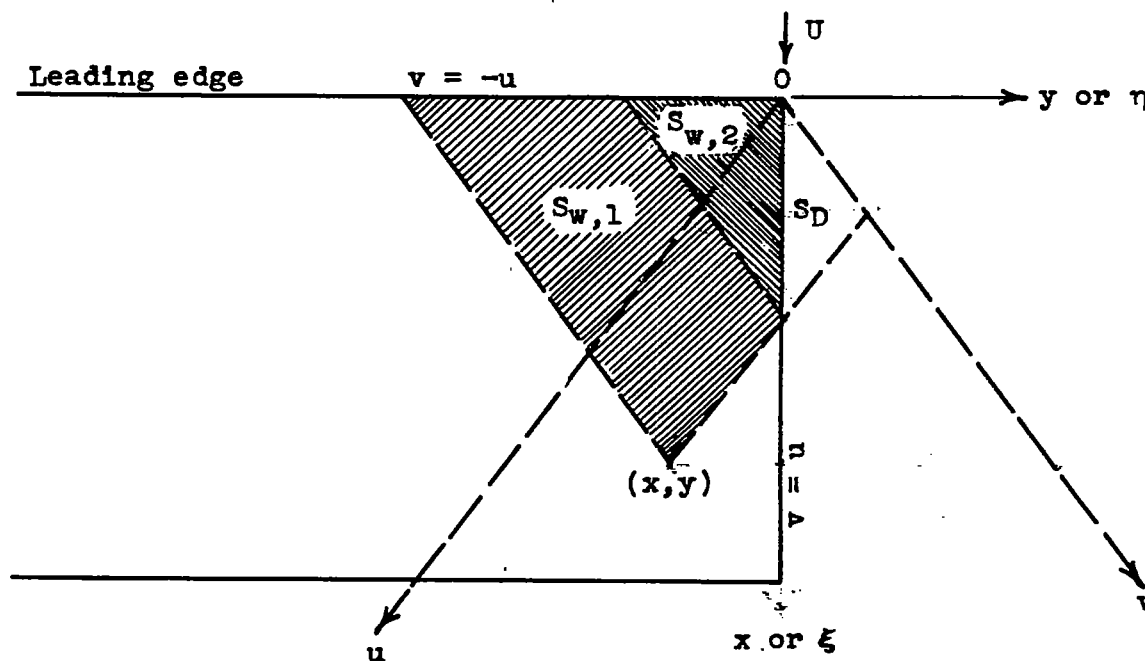   3d rev. ed., 1929, p. 18.
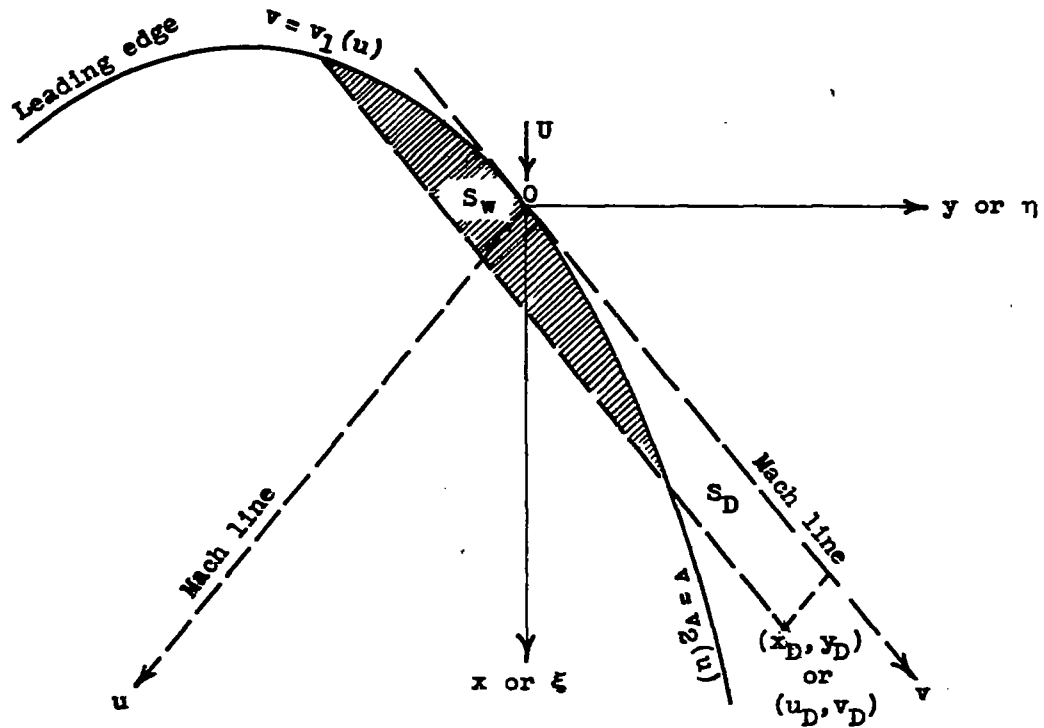
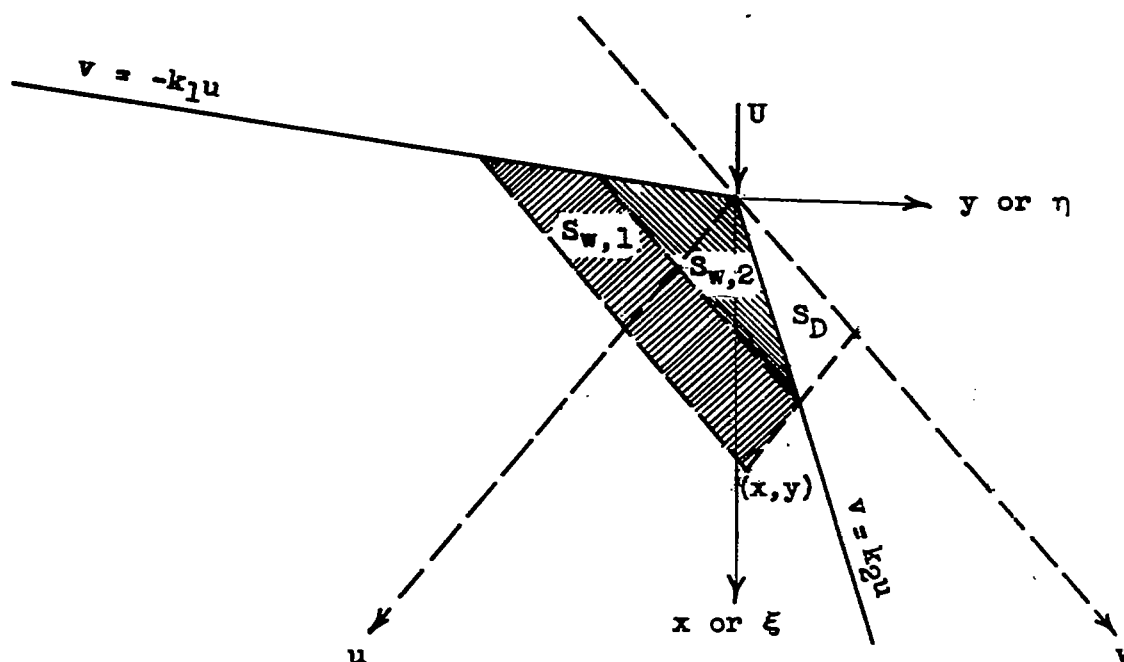(a) Point external to wing surface.
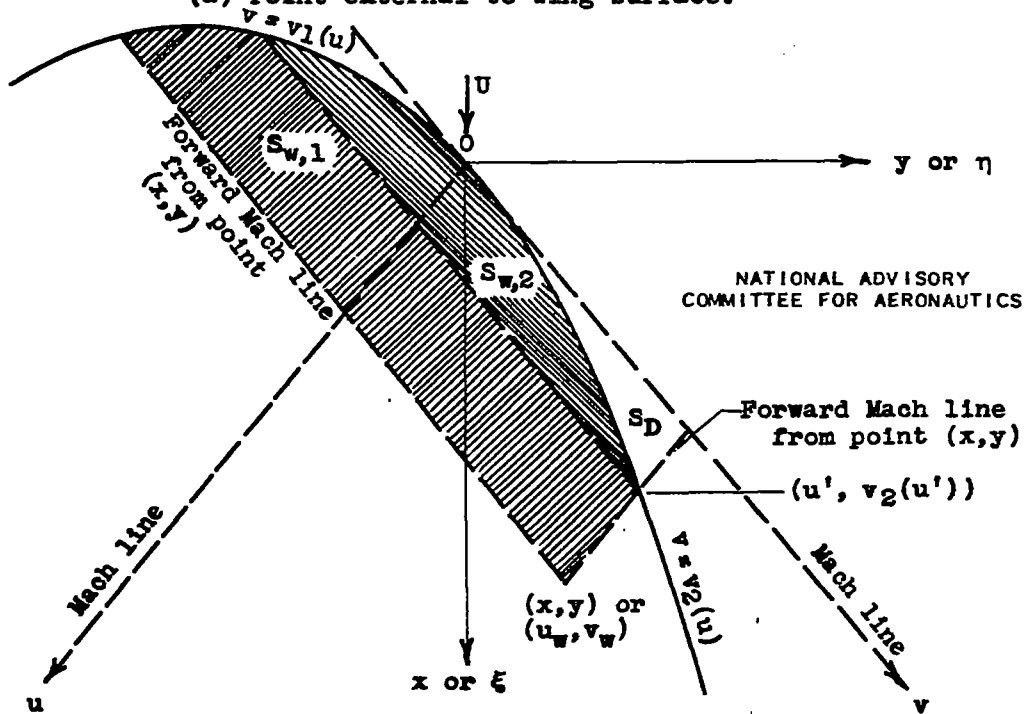
(b) Point on wing surface.

Figure 1.- Regions of integration for calculating velocity
potential on surface of variably swept wing at supersonic
speeds.
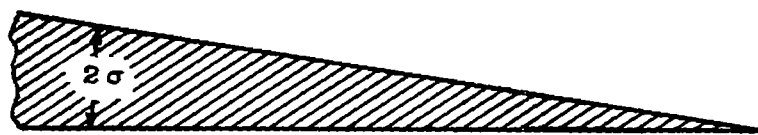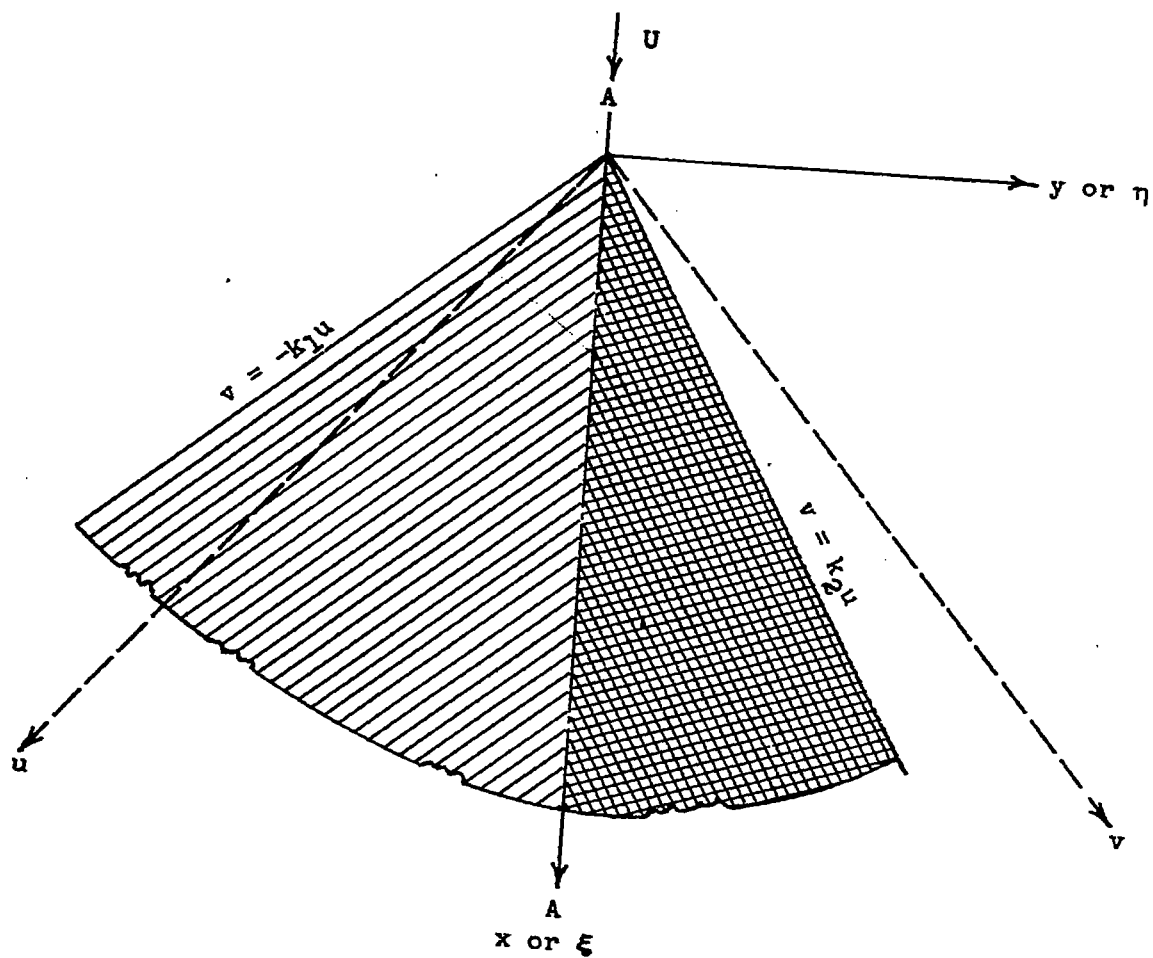
Figure 2.- Integration regions for calculating velocity
    potential on surface of thin flat plate wing at super-
    sonic speeds.

Figure 3.- Regions of integration for calculating velocity
potential on surface of finite thickness, discontinuously
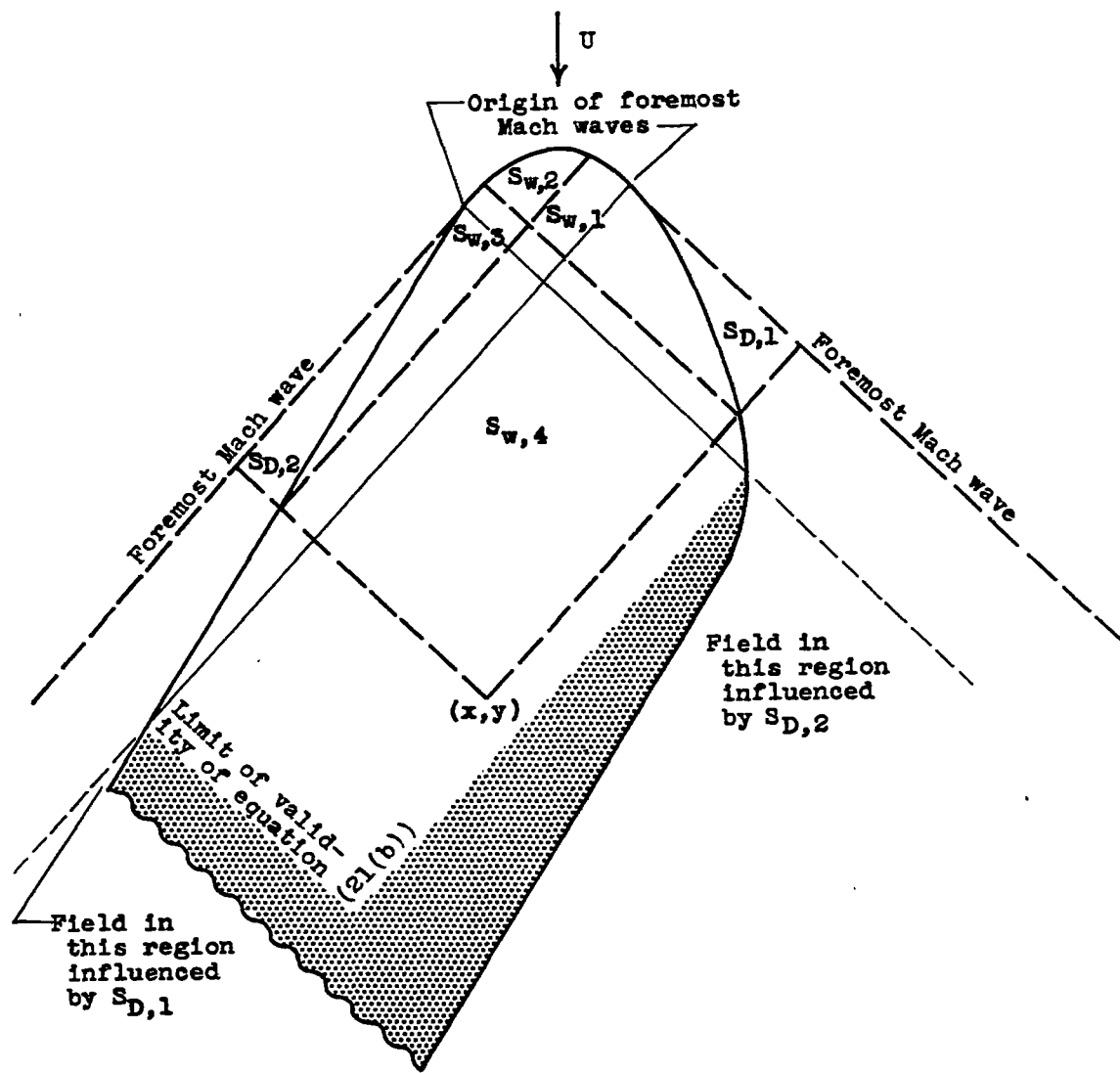swept wing at supersonic speeds.

Fig. 4

U

A

y or η

$v = -k_1u$

u

$v = k_2u$

v

A

x or ξ

2σ

Section A-A

Figure 4.— Discontinuously swept wedge wing.

Figure 5.- Regions of integration for calculating velocity
potential on surface of wing of finite thickness influenced
by two independent perturbed flow fields external to wing
surface.